The Possible Indications of Low-Frequency Gravitational Waves Associated with a Gamma-Ray Burst GRB 051103 in LIGO pre-S5 Data

Abstract. The noise sources of gravitational wave detectors for ground-based laser interferometers by example of LIGO were analyzed. As shown the low-frequency gravitational waves (GW) cause to changes in the detectors' dynamic properties, which manifested as the Q-factor's changes of low-frequency seismic component in a detectors' integral noise that leads to the possibility of indirect GW's observation in the frequency range (~ 100 Hz) of a detectors' extreme sensitivity. The results of public LIGO data associated with gamma-ray burst GRB 051103 and the experimental estimation of GW's properties by results of indirect observation are presented.

Introduction

A registration of the GWs which were predicted in the framework of general theory of relativity (GTR) is significant for the confirmation of the universe's modern physical picture, since the space-time of GTR will cease to be a mathematical model, and will accept the property of the physical object. In addition, the GW observations will provide a lot of additional information about the early stages of the universe's evolution, a development of galaxies and the high-energy processes close to relativistic compact objects [1,2]. Therefore some projects for GW searching were realized. The most successful were projects based on using of ground-based laser interferometers: American project LIGO (Laser Interferometer Gravitational-wave Observatory) and the Franco-Italian project Virgo (the Virgin).

The GW amplitude's measure at laser interferometry is the dimensionless relative deformation h of interferometer's base which was formed between mirrors on the free suspension under the influence of GW. So the laser interferometers can be considered as devices for extremely precise measurements of deformations.

The highest detector's sensitivity was achieved for first phase of the project LIGO (LIGO Initial). But at the target level of detectors' noise the useful signals were not observed.

Noise of interferometers' detectors by LIGO example

For estimating of interferometer's noise the dimensional amplitude $h(f)$ (in $Hz^{-1/2}$) is used. The noise of LIGO four-kilometer detectors L1 and H1 in frequency band of higher sensitivity (100-200)Hz at the final series of measurements was not greater than $3 \cdot 10^{-23} Hz^{-1/2}$, that corresponds to the target parameters of the project. The noise of two-kilometer detectors L2 and H2 is about 8Db higher. Now the LIGO interferometers are rebuilt on an improved version (Advanced LIGO) which must provide noise reduction to $3 \cdot 10^{-24} Hz^{-1/2}$ [3].

The seismic noise (mechanical vibration), thermal noise of mirrors (test masses) and mirrors' suspension, shot noise and radiation pressure are the main sources of detectors ground-based laser interferometers' noise. The amplitude-frequency characteristics of main sources of LIGO detectors' noise are presented in fig.1. The goal characteristic of integral noise for initial LIGO is presented in same figure as a dedicated polyline. The seismic noise

determines the low-frequency part of integral noise. The shot noise determines high-frequency noise of detectors. The integral noise within the maximum sensitivity's domain (100-1000 Hz) is defined by thermal noise of the mirrors' suspension.

The LIGO detectors noise characteristics are unique because the amplitude of mechanical movements of macroscopic objects such as mirrors (mirrors weight ~ 10 kg) is comparable with amplitude of thermal motion of molecules and atoms.
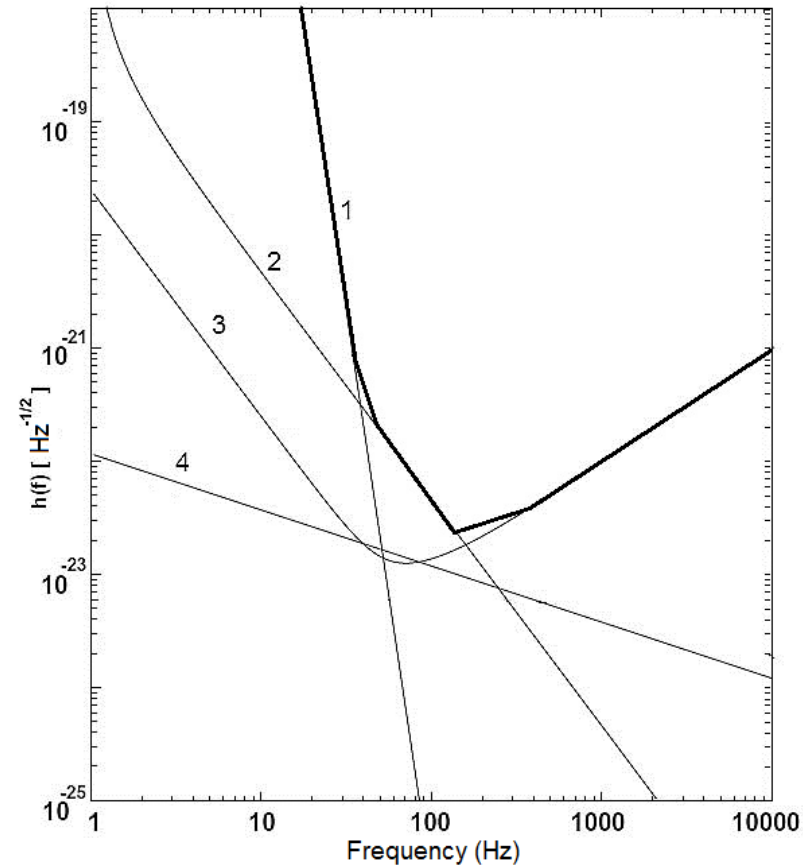
Fig.1. The goal characteristics of the main sources of detectors' noise for Initial LIGO [4]: 1 – seismic noise; 2 – suspension thermal noise; 3 – radiation pressure & shot noise;   4 – test mass thermal noise.

Analysis of the interferometers' signals by LIGO data

In view of the well-known amplitude-frequency characteristics of the potential sources of GW [5.6], the frequency band of LIGO detectors' most sensitive (fig. 1) corresponds to the GW's frequency for the mergers of star-like binary systems with mass $M \sim M_{Sun}$, where M_{Sun} is the mass of the Sun, and for the collapse of Supernovas' external shells. The LIGO detectors are designed for direct registration of GW, with the ability to estimation their polarization (L-shaped configuration of Michelson interferometers) and directions to the source due to distance 3030km between detectors (detectors L1, L2 are in Louisiana, H1, H2 are in Washington State).

Thus the usual strategy of direct primary registration GW is based on some principles:

1. The frequency of potential sources of GW should be in frequency band of detectors' maximum sensitivity 100Hz-1kHz;
2. The signals which were received from different detectors simultaneously should be handled by spectral-correlational methods for comparative analysis;
3. The key criterion of GW registration is a statistically significant relationship between the results of the comparative analysis.

The first condition leads to reducing the number of important potential GW sources available for registration, because the sources with greatest magnitudes of GW such as mergers of intermediate black holes with masses $(10^2 - 10^4)M_{Sun}$ and supermassive black holes with masses $(10^5 - 10^7)M_{Sun}$ have the GW frequencies $(10^{-2}-1)$Hz and $(10^{-5}-10^{-3})$Hz, respectively.

An efficiency of spectral-correlational methods at comparative analysis under the stipulation that the unstable useful signal has a slight excess above the noise is connected with a need of analysis on long time periods (day, week even month and year). Therefore, these methods are suitable for siren-like sources (pulsars, binary systems far off merge), but not for the flashes (mergers of binary systems, collapses). Application of traditional methods of time-frequency analysis which are based on the power estimations to flashes is problematic because useful signal's excess above the background can be observed only on two-three periods of GW.

Comparison of signals of similar detectors at the stage of primary exceedances of the useful signal above the background is problematic too because the detectors' dynamic characteristics on the level of noise are not quite similar.

July 11, 2012 the comprehensive report based on the results of the study of the relationship between the short gamma-ray burst GRB051103 [7] and synchronous measurements of the gravitational wave magnitude by LIGO's L1 and H2 detectors (run pre-S5) was published on the LIGO's Document Control Center website [8]. The report was accompanied with publication of the measurements' data: strain registration by detector H2 (H2-STRAIN_16384Hz-815043278-2190 and H2-STRAIN_4096Hz-815045078-256), strain registration by detector L1 (L1-STRAIN_16384Hz-815043278-2190 and L1-STRAIN_4096Hz-815045078-256) and noise spectrum for the detectors, related to the same time. According to file name data sampling rate were 16384S/s (samples per second) or 4095S/s, the recording duration 256s or 2190s and sampling beginning time GPS815043278 (03.11.05 08:54:25 GMT) or GPS815045878 (03.11.05 09:24:25GMT). Additionally, in the description of the report [8], it was reported that the data with sampling frequencies 16384Hz and 4095Hz are the result of high-pass filtering source data with cut-off frequencies 20 Hz and 30 Hz,

respectively, in order to reduce the influence of the dominant seismic noise. Thus we had possible to analyze the real signals of LIGO detectors after standard prehandling.
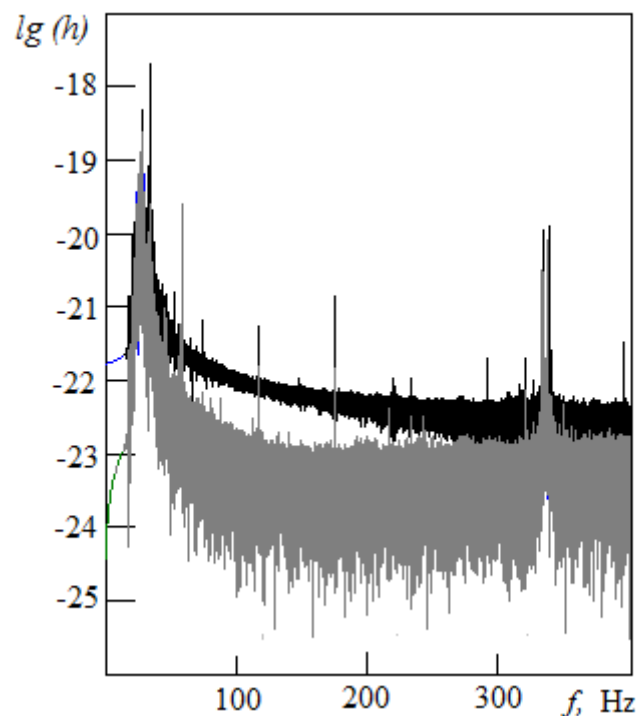
Fig.2. Spectrums of signals H2-STRAIN_4096Hz-815045078-256 (black) и L1-STRAIN_4096Hz-815045078-256 (gray).

We had compared the two signals obtained with different LIGO detectors which were handled by similar modes of digitization and filtering: H2-STRAIN_4096Hz-815045078-256 and L1-STRAIN_4096Hz-815045078-256. Figure 2 presents the spectrums of the signals received during all time of observing (256s). Signals' spectrums correspond to the spectrum of seismic noise which contains the dominant harmonic with frequency about 30Hz and with random amplitude.

In the frequency band of greatest sensitivity (100-200 Hz) the largest difference between spectrums there is. The spectrum of detector L1 is close to integrated target characteristic of the noise (fig. 1) with a local minimum in the band of greatest sensitivity, where spectrum is formed by the

suspension's thermal noise. In the spectrum of detector H2 the suspension's thermal noise is suppressed by dominant harmonic of seismic noise. That is connected not only with greater amplitude of the harmonic, but with lesser Q-factor (quality factor) of seismic noise for the detector H2.
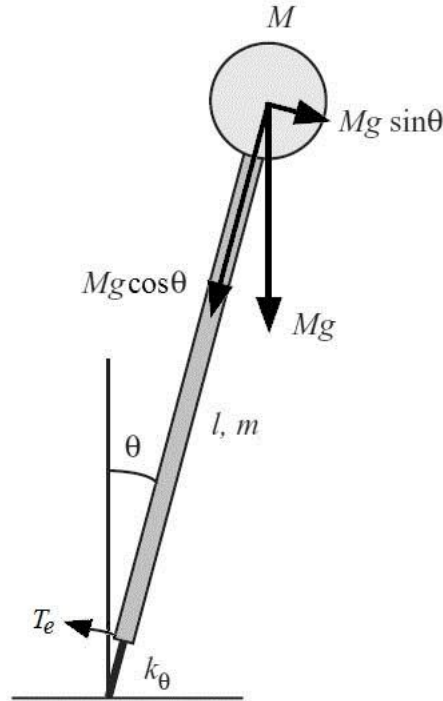
Fig.3. Dynamic scheme of the invert pendulum: k_θ – torsion rigidity of absorbers; T_e - elastic moment; M,m,l – lumped mass, distributed mass and length of pendulum respectively.

Source of the LIGO detectors' seismic noise at frequency ≈ 30 Hz is the multistage suspension of test masses (mirrors) under an influence of random seismic movements (grounds, atmosphere, ocean, industrial activity and other) [4]. Mirrors are suspended on the frame using steel wire. The frame is mounted on elastic shock absorbers. The dynamic scheme of the frame on the elastic shock absorbers can be presented as invert pendulum (Figure 3). Q-factor of the pendulum can be written as

$$Q=l^2(k_{eff}/k_\theta)Q_{int}, \qquad\qquad (1)$$

where $k_{eff} = (k_\theta /l^2) - (m/2 +M)g/l$ – effective rigidity of pendulum taking into account the gravitational force; Q_{int} – intrinsic pendulums' Q-factor which are determined by damping properties of absorbers and environment's damping influence [9].

The equation (1) shows that the Q-factors of the same type pendulums which have the different locations can be different, because the local values of the gravitational acceleration can be different too. In addition, the elastic-dissipative properties of structurally similar shock absorbers can be various and unstable. The first registration of useful signal at the level of the utmost sensitivity can be achieved on detector with the least level of noise therefore the statistical and dynamical criteria of a registration's verification which are based on a large number of theoretical works [10,11,12,13,14] aimed at establishing the GW forms take on special significance.

In the papers [15,16] we have proposed and approbated high-sensitivity method of analysis for detection of harmonic and quasiharmonic signals amid the random noise. The method is based on a comparison between signal's waveform and sine wave with analyzed frequency, regardless of signal's amplitude. Proposed method was called form-analysis. The result of analysis for digital signals is a two-dimensional matrix $I_f (m, n)$, each element of which is form-index $I_f (m, n)$, where m,n is analyzed period and time in samples. The form-index is a non-dimensional measure of similarity between signal's waveform at time n and sine wave with period m. The form-index has maximum value 3 for pure harmonics with period m and minimum value -1 (background) for signals with non-harmonic waveforms.
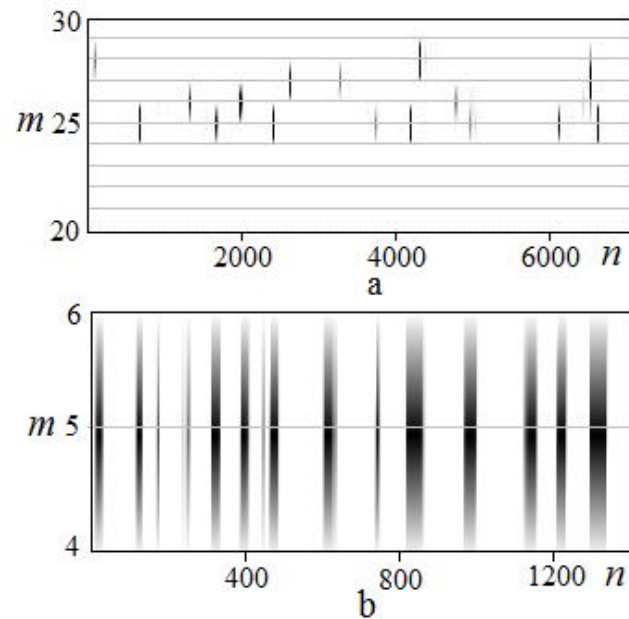
Fig.4. Results of form-analysis for the arbitrary part of the signal
L1-STRAIN_4096Hz-815045078-256

Figure 4a presents the results of analysis for arbitrary part of signal L1-STRAIN_4096Hz-815045078-256 with duration in 7500 samples (~ 1,83s) and with periods from interval 20-30 samples (4,9-7,3ms). The form-factor exceeded over the background value only in periods' interval m = 24-29 (5,9-7,0ms), which corresponds to the frequency range of 140-170Hz.

Taking into account the properties of the form-analysis the registration significant form-factor in the frequency band 140-170Hz can be bound up with presence in the band the physically implemented vibrations which are independent from detector's seismic noise. These vibrations can be considered as a useful signal only in terms of its differences from the nature of detector's basic noise. The observed vibrations by type of manifestations can be attributed as detector's thermal noise (fig.1).

For bringing information about useful signal's properties to only one non-dimensional parameter resampling of signal L1-STRAIN_4096Hz-815045078-256 with sampling rate 820S/s was fulfilled after the procedure of low-pass digital filtration. As a result the resolution of analysis was reduced fivefold. In Figure 4b presents that after resampling all information about the useful signal gone in band $m=5$ (period 6, 1ms, frequency about 160Hz). The dynamics of form-index of useful signal in that band corresponds to stationary random process.

In Figure 5a presents the results of analysis of signal L1-STRAIN_4096Hz-815045078-256 after resampling on full time interval 256s. On long time intervals the form-index remains stationary, but on relatively short time intervals (windows-like) the form-index is reduced until background values (-1) that corresponds to a rapid decrease in useful signal-to-seismic noise ratio. Comparison of signal start time with time short gamma-ray burst GRB 051103 indicates that the gamma-ray burst occurred 79s after the start of the recording (in Figure 5 the time gamma ray burst is marked as a black arrow on the timeline). Gamma-ray burst is exactly concurring with front border of second window. This coincidence may be not accidental, since the gamma-ray burst was very short (17ms) and throughout the signal (256s) only two windows with explicit front border is observed.

Fig.5. Results of form-analysis of the signal
L1-STRAIN_4096Hz-815045078-256 on full time interval

In Figure 5a presents the results of analysis of signal L1-STRAIN_4096Hz-815045078-256 after resampling on full time interval 256s. On long time intervals the form-index remains stationary, but on relatively short time intervals (windows-like) the form-index is reduced until background values (-1) that corresponds to a rapid decrease in useful signal-to-seismic noise ratio. Comparison of signal start time with time short gamma-ray burst GRB 051103 indicates that the gamma-ray burst occurred 79s after the start of the recording (in Figure 5 the time gamma ray burst is marked as a

black arrow on the timeline). Gamma-ray burst is exactly concurring with front border of second window. This coincidence may be not accidental, since the gamma-ray burst was very short (17ms) and throughout the signal (256s) only two windows with explicit front border is observed.

Interrelation between short gamma-ray bursts and gravitational waves derives from some physical models of GRB's origin which are based on coalescence of compact objects in binary systems [17]. If the speed of gravity waves equal to the speed of light in vacuum, a synchrony between gamma-ray bursts' and gravitation waves' registration must be observe. By analogy, we can assume that non-stationarity in the process (fig. 5a) associates with relatively slow changing of detector's dynamic properties which is caused changing space-time properties (metric) as result of incoming gravitational waves associated with a process of gamma-ray burst generating. Since seismic noise detector is the monochromatic signal with random amplitude we can assume as first approximation that with the arrival of gravitational waves a Q-factor of the seismic noise is reduced.

At lower values of form-index in the windows a decrease of form-index dispersion there is too. The Figure 5b presents the form-index dispersion's value during observation time in decibels relative to the maximum value. The lowest dispersion values occur in area of the windows' bottoms, but the dispersion axis on the Figure 5a was turned to traditional format, in which the gravitational wave magnitude increase corresponds to the visual increase of estimation parameter (dispersion).

The gamma-ray burst GRB 051103 belongs to the gamma-ray bursts with known direction to the source. The most likely source of the burst was in a group of actively interacting galaxies M81/M82/NGC3077, located at a distance of 3.6 Mps (12 million light years) from Earth [18]. Interest to GRB 051103 as a potential source of gravitational waves was connected, firstly, with the relative proximity of galaxies groups M81/M82/NGC3077 to Earth and, secondly, with the ability to generate large-amplitude gravitational waves in the course of astrophysical processes (coalescence) by generating of short gamma-ray bursts.

The Fig. 6 presents a qualitative scheme of gravitational waves generation during the process of compact binary objects' coalescence by K. Thorne [10]. The coalescence is begun by a lengthy stage of inspiral (1) that ends with the last stable circular orbit. In some papers [11,12] the final stage of the inspiral is called plunge. After passing the event horizon there comes a merger stage (2) that ends with the formation of a rotating Kerr black hole. At ringdown stage (3) a magnitude gravity waves of Kerr black hole rapidly decreases without frequency changing.

The coparison Fig.5b and Fig.6 shows a quality similarity between waveforms. Similar parts of waveforms in figures was marked by vertical arrows, which allow to mark of coalescence stages. The first two high waves in Figure 5b belong to inspiral stage and the last three waves belong to ringdown stage.
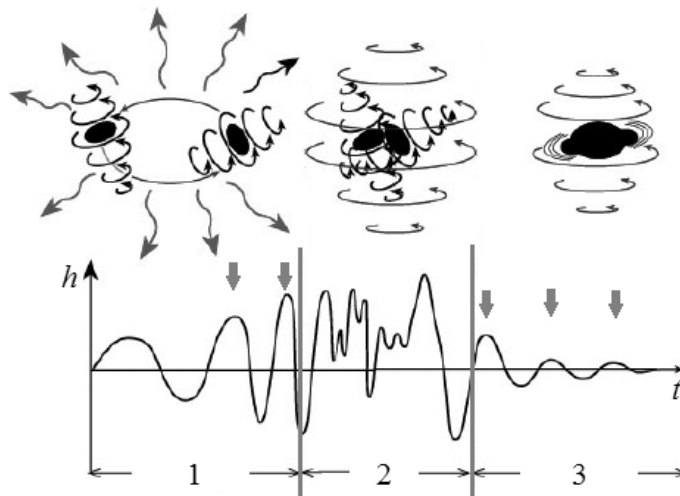
Fig.6. Estimating gravitation wave-form from binary coalescence

Waiting the project LISA (Laser Lisa Space Antenna) realization the binary objects as sources of low-frequency gravitational waves have been the subject of a lot theoretical studies [11, 12, 13, 14], based on the numerical simulation of the coalescence dynamics. The quantitative estimations of gravitational wave's parameters for different types of compact objects at inspiral stage and at ringdown stage were received. At merger stage the coalescence's processes are chaotic, so the parameter of gravitational waves and duration of the stage are not known [10].

The Figure 7 presents the results of a simulation of the coalescence of two compact rotating objects with mass ratio 1: 4 [13]. The legs of theoretical waveform corresponded to results of analysis (fig. 5b) are shown by vertical arrows. At merger stage the theoretical waveform is absent by reason of both theoretical and computational complexities of modeling. In the system $G = c = 1$ time is measured in $M = 5 \cdot 10^{-5}$ (M/M_{Sun}) c, where M is the total mass of coalesced objects; M_{Sun} is the mass of the Sun. Time scale's zero corresponds to the transition of a smaller object through the event horizon.
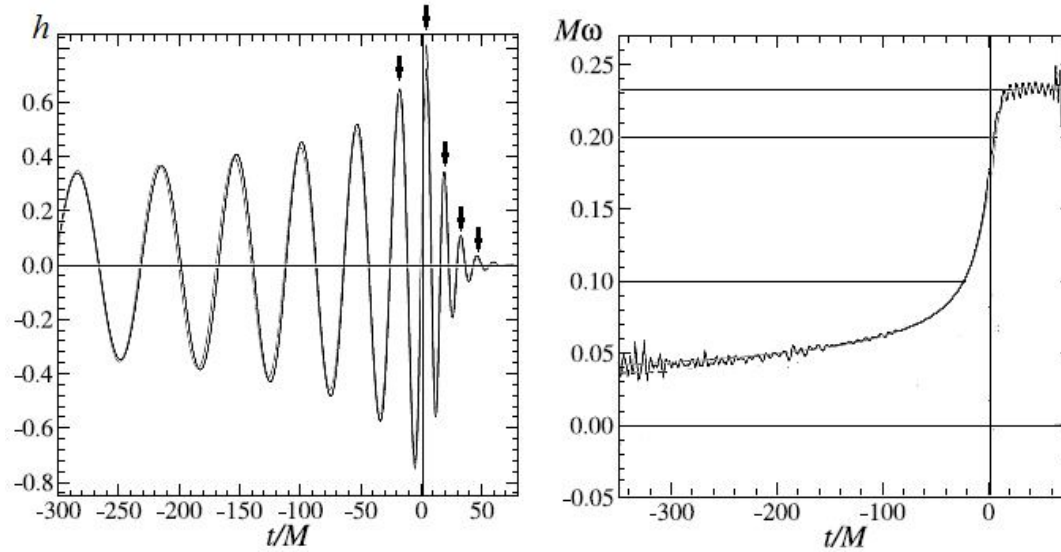
Fig.7. Results of the wave-form modeling

By comparing figures 5b and 7 an estimate of the total mass of the coalesced objects may be made. At ringdown stage $M\omega = 0.23$, where ω is the angular frequency of objects' rotation which is two times less than gravitational waves' frequency. In Fig. 5b wave's period at ringdown stage $T_{ring} = 40$ c, so the total mass of objects:

$$M = (M\omega) \cdot 2T_{ring} \cdot (2\pi)^{-1} = 0{,}23 \cdot 80/6{,}28 = 3c = 6 \cdot 10^4 \ M_{Sun}.$$

According to the estimation and by the model presented in Figure 7 the mass of small object is 12000 M_{Sun}, and the mass of large object 48000 M_{Sun}. The objects of such mass can be the black holes only, but their mass is less than the mass of the supermassive black holes ($10^5 \ M_{Sun}$) and much more than the mass of stellar-like black holes. The estimated mass is not typical for black holes, but compact objects with middle mass were observed in X-ray range by telescope Chandra. The compact objects in the Galaxy M82 have masses in range from 12000 M_{Sun} to 43000 M_{Sun} [19].

In GTR the GW are considered as waves of space-time continuum [1,2]. The space-time of GTR is a magnificent mathematical model of gravitational field but space-time cannot be considered a physical substance for transmission of GW. The substance transmitting the GW is the space vacuum [20]. The equality speed of GW with speed of light (fig. 5) corresponds to a "quintessence" (a sort of dark matter) as the model of space vacuum [21]. As noted R. Cardwell in paper [22], "the vacuum is not rigid, but instead is susceptible to fluctuations driven by gravity". Therefore GW can be considered as the waves of pressure in accordance with state equation $p = w\rho$, where ρ is the density of vacuum energy; $w = -1$ for the standard quintessence model.

Analysis of the expression (1) shows that at the expected values of GW's magnitudes the effective stiffness and torsion stiffness of inverse pendulum remain constant and Q-factor can be changed only by changing the pendulum's intrinsic Q-factor (Q_{int}), which depends on the influence of an environment. The test masses of interferometers are constructively in high vacuum therefore the environment for mirrors in adopted model is the quintessence. The damping properties of quintessence will increase with increasing of vacuum energy under influence of GW in accordance with state equation. Then the Q-factor of seismic noise under influence of GW will decrease. The effect must appear primarily on the steep leading edge of shock waves from mergers of massive binary systems, as observed in the experiment.

Conclusion

The most perspective sources for detection of GW are mergers of black holes in binary systems with a total mass exceeding 10^4 M_{Sun} . The frequency of such events is less than 10^{-2}Hz that is outside the work frequency band of the existing ground-based interferometers (100-1000) Hz.

Change of the environment's properties under influence of GW can manifest itself in changing of the dynamic properties of the detectors. In particular, with the change of damping environment's properties as a result of changing the vacuum energy's density under action of GW the Q-factor of the detector's seismic noise can be changed too. Taking into account the combined nature of detectors' noise the registration of GW can be based on an analysis of the relationship between mechanical and thermal noise of the detectors. The low-frequency GW will manifest itself as low-frequency changes of dynamic properties of detectors.

For use of such approach the seismic noise of interferometer's sensor must has high initial Q-factor and the main frequency of seismic noise f_S must be many larger than the frequency of GW f_{GW} ($f_S \gg f_{GW}$). In connection with these conditions the investigation of the high-level quality nanomechanical systems [23] to identify slow systematic changes Q-factor has interest.

The list of references

1. Grishchuk L.P., Lipunov V.M., Postnov K.A. et al. Gravitation-wave astronomy: in waiting of first registered source // UFN. – 2001. – V.171. - №1. – P.3–59 (in Russian).

2. Mizner Ch., Thorne K., Wheeler J. Gravitation: trans. from Eng. in 3v. M.: Mir, 1977. V. 3. P.161(in Russian).

3. Pitkin M., Reid S., Rowan S. et al. Gravitational wave detection by interferometry (ground and space) // Living Rev. Relativity. – 2011. – V.14 – P. 5.

5. Thorne K.S. Gravitational radiation // Three hundred years of gravitation: ed. by Hawking S.W., Israel W. Cambridge: Cambridge University Press, 1987. P. 330.

6. Blair D.G. Sources of gravitational waves // The detection of gravitational waves: ed. by Blair D.G. Cambridge: Cambridge University Press, 2005. P. 16.

7. Golenetskii S., Aptekar R., Mazets E. et al. GCN Circular #4197, NASA. URL: http://gcn.gsfc.nasa.gov (date of address: 23.07.13).

8. LIGO Data Release associated with GRB051103 (LIGO Document P1200078-v4). URL:https://dcc.ligo.org/cgi-bin/DocDB/ShowDocument?docid=93109 (date of address: 22.07.13).

9. Tacamori A., Raffai P., Marka S. et al. Inverted pendulum as low-frequecy pre-isolation for advanced gravitational wave detectors // Nuclear Instruments and Methods in Physics Research Section A. – 2007. – V.585. – Issue 2. - P. 683-692.

10. Thorne K.S. Black holes and time warps: Einstein's outrageous legacy. M.: Physmatlit, 2007. P. 396 (in Russian).

11. Taracchini A., Pan Y., Buonanno A. et al. Prototype effective-one-body model for nonprecessing spinning inspiral-merger-ringdown waveforms // Phys. Rev. D. – 2012. – V.86. – id.024011.

12. Buonanno A., Damour T. Transition from adiabatic inspiral to plunge in binary black hole coalescences // Phys. Rev. D. – 2000. – V.62. – id.064015.

13. Baker J. G., Centrella J., Choi D.-I. et al. Binary black hole merger dynamics and waveforms // Phys. Rev. D. – 2006. – V. 73. – id.104002.

14. Buonanno A., Pan Yi, Baker J. G. et al. Toward faithful templates for non-spinning binary black holes using the effective-one-body approach // Phys. Rev. D. – 2007. – V.76.– id.104049.

15. Prygunov A.I. A new tool for experimental investigation of chaos: theory and applications // Vestnik MSTU. – 2008. – V. 11. - №3. – P.379-384. URL: http://vestnik.mstu.edu.ru/v11_3_n32/articles/02_pryg.pdf

16. Prygunov A.I. An experimental exploration of the dynamical chaos' structures // Vestnik MSTU. – 2010. – V. 13. - №4/2. – P.1092-1098. URL: http://vestnik.mstu.edu.ru/v13_5_n42/articles/45_prygun.pdf

17. Nakar E. Short-hard gamma-ray bursts // Phys. Rep.(Rev. Sec. of Phys. Lett.). – 2007. – V. 442(1-6). – P. 166-236.

18. Frederiks D.D., Pal'shin V.D., Aptekar' R.L. et al. On the possibility of identification of a short/hard burst GRB 051103 with the giant flare from a soft gamma repeater in the M81 group of galaxies. URL: http://arxiv.org/pdf/astro-ph/0609544v3.pdf (дата обращения: 23.07.13).

19. Feng H., Rao F., Kaaret P. Discovery of millihertz X-ray oscillations in a transient ultraluminous X-ray source in M82 // Astroph. Jour. Let. – 2010. – V.70. – P. 137-141.

20. Chernin A.D. Space vacuum // UFN. – 2001. – V.171. - №11. – P.1153–1175 (in Russian).

21. Erickson J. K., Cardwel R.R., Paul J. et al. Measuring the speed of sound of quintessence // Phys. Rev. Lett. – 2002. – V.88. – id.121301.

22. Cardwell R.R. Gravitation of the Casimir effect and the cosmological non-constant. URL: http://arxiv.org/pdf/astro-ph/0209312.pdf (date of address: 23.04.14).

23. Bagci T., Simonsen A., Schmid S. et al. Optical detection of radio waves through a nanomechanical transducer // Nature – 2014. - V 507. – P. 81-85.

Supplementary information to the article
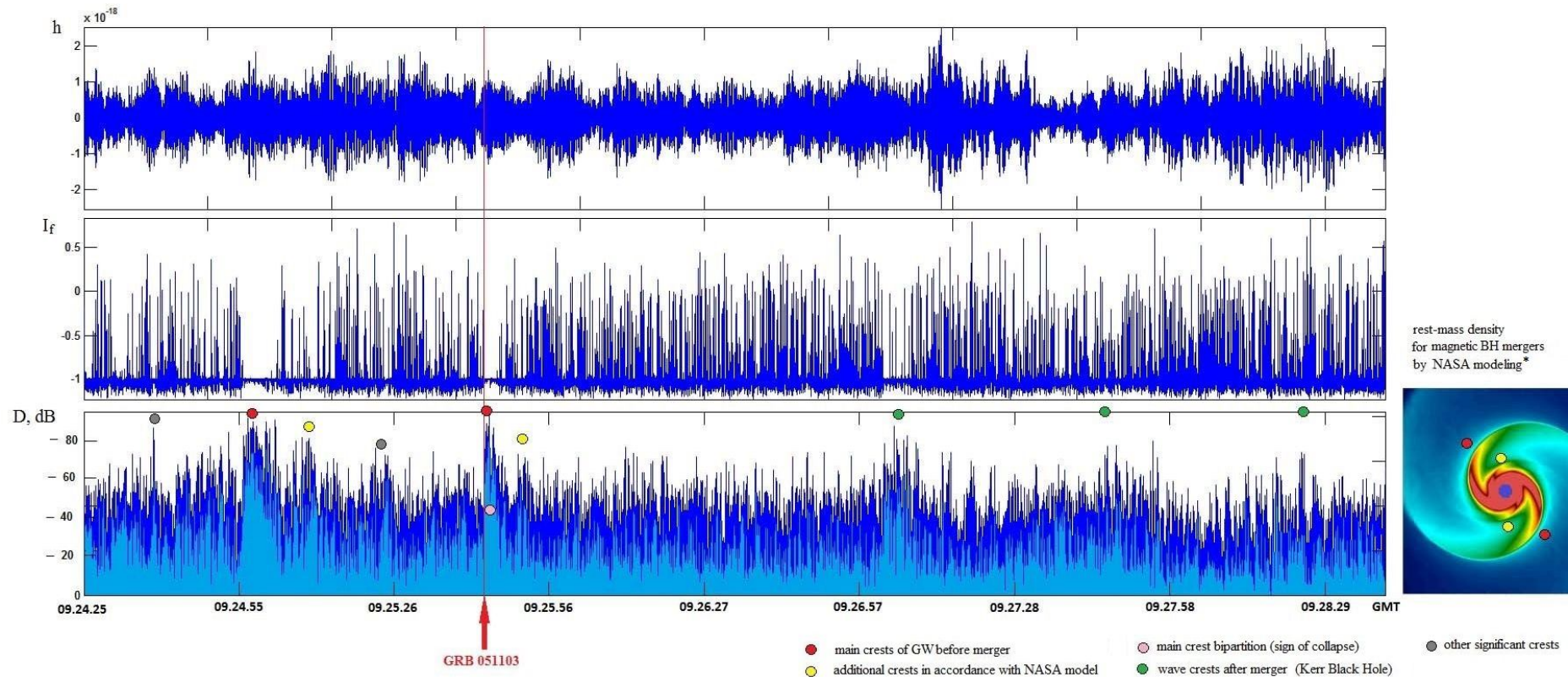
* Giacommazzo B., Baker J. G., et al. General relativistic simulation of magnetized plasmas around merging supermassive black holes // arXiv:1203.6108v2 [astro-ph.HE] 15 May 2012

Link to download of digital data (h,D,If) as MATLAB MAT-file https://yadi.sk/d/O46vznuscKtZh